Polymer Testing **11** (1992) 271–288

Fracture Toughness Determination of ABS Polymers Using the *J*-method

Celina R. Bernal, Patricia M. Frontini*

Institute of Materials Science and Technology (INTEMA), University of Mar del Plata and National Research Council (CONICET), J. B. Justo 4302, 7600 Mar del Plata, Argentina

&

Ruben Herrera

Center for Industrial Research, Fudetec, Dr Jorge Simini S/N, 2804-Campana, Argentina

(Received 9 September 1991; accepted 2 October 1991)

SUMMARY

The suitability of J–R *curve fitting methods proposed by ASTM E* 813-81 *and E* 813-87 *metal standards in fitting ABS* J–R *curves is discussed. Tests were carried out at room temperature on one commercial grade ABS resin in three-point bending.*

*Specimens were precracked with a razor blade and tests were performed over a X*20 *range of crosshead rate in the quasistatic regime.*

Specimens of different geometric relationships (B/W, a/W, *smooth specimens of different thickness, and side-grooved specimens*) *were assayed.*

The two ASTM fitting procedures were also checked against data reported by other authors for other ABS type resins.

Model appropriateness was checked by statistical analysis.

Results appeared to be geometrically independent for deeply notched specimens. No significant variation in the J–R *curve was found for changes in the displacement rate. Both* J-R *curve fittings appeared to be adequate.*

The ASTM E 813-87 *procedure led to less conservative critical initiation* J_{IC} *values.*

* To whom correspondence should be addressed.

Polymer Testing 0142-9418/92/$05·00

1 INTRODUCTION

ABS type resins are two-phase materials consisting of elastomer particles in a glassy polymer matrix.

These materials exhibit nonlinear elastic behavior under the test conditions studied in this paper. Hence, the use of a fracture criterion considering this behavior is necessary.

One such scheme is the J-integral first proposed by Rice,[1] which is a nonlinear elastic approach widely used for materials that exhibit elastoplastic behavior, as in the case of metals.

For polymers, nonlinearities arise from viscoelasticity. In the last decade, however, this approach has been successfully applied to polymers with the following precautions:[2] performing the analysis at constant strain rate under increasing monotonic loads without unloading during the test. This approach has also been applied to ABS type resins specifically.[3–5]

However, a number of questions remain unanswered in the application of fracture mechanics to the testing of a tough thermoplastic. With the increase in structural use of thermoplastics such as ABS, the need has arisen for a method to determine useful fracture mechanics parameters for failure prediction.

As there is no currently approved standard for determining the fracture toughness of thermoplastics, authors based their measurements on the procedures developed for metals, more specifically on ASTM E831–81 and E831-87 standards.

The main difference between these standards is the material J resistance (J–R) curve adjustment method proposed, and the determination of the critical initiation fracture parameter J_{IC}. The former method proposes an extrapolation of J value at initiation and the latter an engineering value corresponding to a fixed displacement value.

This investigation aims to:

—obtain valid ABS J–R curves using unsophisticated devices;
—assess the two fittings proposed for both standards when adjusting ABS J–R curves;
—compare the critical initiation values (J_{IC}) obtained from both procedures;
—study the influence of geometry relationships and test conditions upon the J–R curve and J_{IC}.

2 MATERIALS AND SPECIMENS PREPARATION

A commercial grade ABS type Resin (Lustran ABS HR 850, Monsanto Argentina S.A.) was used. Pellets of ABS resins were dried at 85 °C for

2 h under vacuum and then compression moulded at 195 °C into thick plates.

In order to release the residual stresses generated during moulding all the plaques were submitted to a postmoulding thermal treatment consisting of keeping the samples for 1 h at 120 °C under a slight pressure and then slowly cooling to room temperature.

Fracture characterization was carried out on three-point bend specimens (SENB), cut out from the compression-moulded plates (thickness between 4·5 and 9·5 mm) and manually sandpapered to improve the edge surface finish of each specimen.

Sharp cracks were introduced by machining with a sharp fly cutter. 'Crack to depth ratio' (a/W) was varied between 0·3 and 0·8. The 'thickness to depth ratio' (B/W) used was of 0·2, 0·5 or 1. 'Span to depth ratio' (S/W) was always kept equal to 4.

One set of specimens, 7 mm thick, was side-grooved, reducing the thickness by 20%. The angle of the side grooves was 45°. Specimens were side-grooved before sharp notching.

Both specimen configurations, smooth and side-grooved, are shown in Fig. 1(a) and (b).

The dumb-bell specimens for yield stress determination were cut from 3 mm resin plaques in accordance with the ASTM D638-type I description.

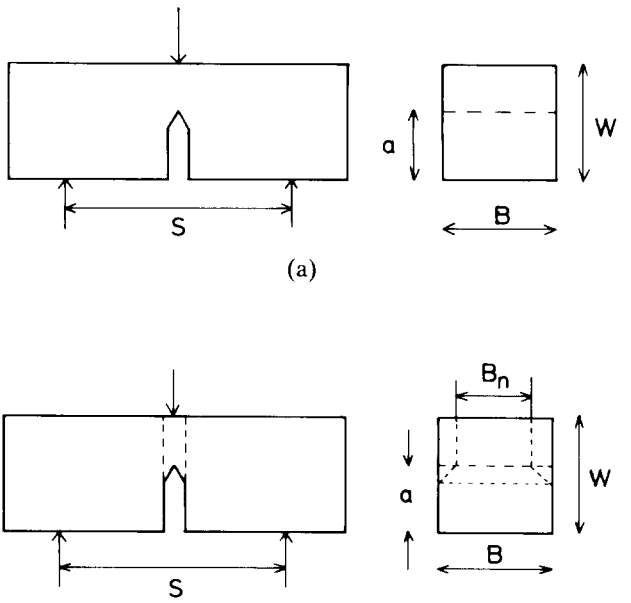

Fig. 1. Specimen configuration: (a) smooth type; (b) side-grooved type.

3 EXPERIMENTAL PROCEDURE

3.1 Method

J-resistance curves were determined by the multiple-specimen technique, first proposed by Landes and Begley,[6] consisting of loading a series of identical specimens to various subcritical displacements, producing different amounts of crack extension, Δa

The value of J for each specimen was determined from the load versus displacement curve by the approximate equation proposed by Rice *et al.*[7]

$$J = \frac{2U}{B(W-a)}$$

which is valid only for S/W equal to 4 and a/W between 0·4 and 0·7. The fracture energy, U, is the area under the load deflection curve. J–R curves were constructed by plotting values of J as a function of Δa.

3.2 Fitting of J–R curves

J–R curves were then fitted following two different procedures recommended by the two metal standards ASTM E813-81 and ASTM E813-87, respectively. The first standard proposes a bilinear approximation of the J–R curve. The first line, called 'the blunting line' represents the blunting behavior of the crack tip before real crack propagation. It has an analytical expression:

$$J = 2\sigma_y \, \Delta a$$

assuming a blunted crack with a semicircular profile.

The second line is fitted to experimental stable crack growth data.

The crack initiation value J_Q, is taken to be the critical crack initiated value in mode I where the two lines intersected.

On the other hand, the second standard proposes an exponential J–R approximation fitting data points by a power law:

$$J = C_1 \, \Delta a^{C_2}$$

The initiation value J_Q was now at the intersection of the power law and a 0·2 mm offset line parallel to the blunting line:

$$J = 2\sigma_y(\Delta a - 0{\cdot}2)$$

For both standards the crack initiation value J_Q is set to be J_{IC} (plane strain critical initiation value in mode I) if the following size conditions

are met

$$B,\ W-a>25\frac{J_Q}{\sigma_y}$$

$$\frac{dJ}{da}<\sigma_y \quad \text{(for ASTM E813-81)}$$

or

$$\left.\frac{dJ}{da}\right|_{\Delta a_Q}<\sigma_y$$

where Δa_Q is the crack growth corresponding to the crack initiation point for ASTM E813-87. Both procedures are shown schematically in Fig. 2.

In what follows we will call $J_{IC\text{-}81}$ the J_{IC} value calculated following ASTM E813-81 specifications and $J_{IC\text{-}87}$ the one calculated by ASTM E813–87 specifications.

3.3 Exclusion lines

For three sets of specimens (4·5, 7 and 9·5 mm thick) the resistance curve was fitted, choosing valid data points by three different criteria:

—Using every data point obtained in the tests (except the ones belonging to the blunting line when ASTM E813–81 procedure was used).

—Using only data points where crack growth was between two offset lines drawn parallel to the blunting line. The minimum offset was 0·6% of the ligament and the maximum offset was 6% of the ligament, as Huang and Williams[8] recommend.

—Using only data points where crack growth was between two offset lines drawn parallel to the blunting lines that are offset by 0·15 and 1·5 mm, as the ASTM standards recommend.

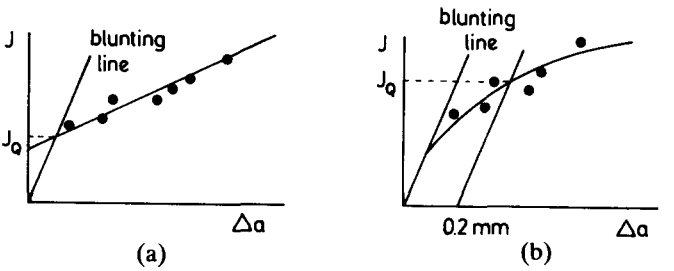

Fig. 2. *J–R* curve fittings: (a) linear fitting; (b) power law fitting.

3.4 Testing conditions

Fracture tests were performed in a Shimadzu Autograph Universal Testing machine S-500-C at room temperature at a constant crosshead speed of 2 mm/min, except for 'crosshead rate influence' experiments where the rate was varied between 0·5 and 10 mm/min.

The marking of crack growth was obtained by painting the fractured surface with an alcoholic solution of iodine before unloading.

The tested specimens were completely fractured after the paint had dried, in a Charpy pendulum at room temperature or, alternatively, first cooled down in liquid air so that the amount of crack extension could be measured from the surface using a profile projector (10×).

According to ASTM E813-81 and ASTM E813-89 specifications the crack front was measured at nine points. Δa was calculated, averaging the near-surface measurements, combining the result with the remaining seven crack extension length measurements, and determining the final average.

The yield stress was taken to be the ultimate stress measured in tension at the same displacement rate used in the corresponding fracture test. This yield criterion seems to be more appropriate for polymers[9] than the one suggested in ASTM standards for metals.

4 RESULTS AND DISCUSSION

4.1 Crack growth measurements

Figure 3(a) shows a photograph of a typical fractured surface of the room temperature pendulum-broken samples. It is possible to appreciate the difference in roughness between the region corresponding to the machined notch and the whitened stress surface where the crack had grown progressively through the predeformed material. The first 'mark' on the whitened surface corresponds to the crack extended under controlled conditions, Δa, and the subsequent mark corresponds to an additional crack advance produced before unloading while the ink was drying.

Figure 3(b) shows the surface of a liquid air-cooled pendulum-broken sample. It is also possible to appreciate the machined notch and the whitened stress surface where the crack had grown progressively through. However, as can be expected in this case, the stress whitened

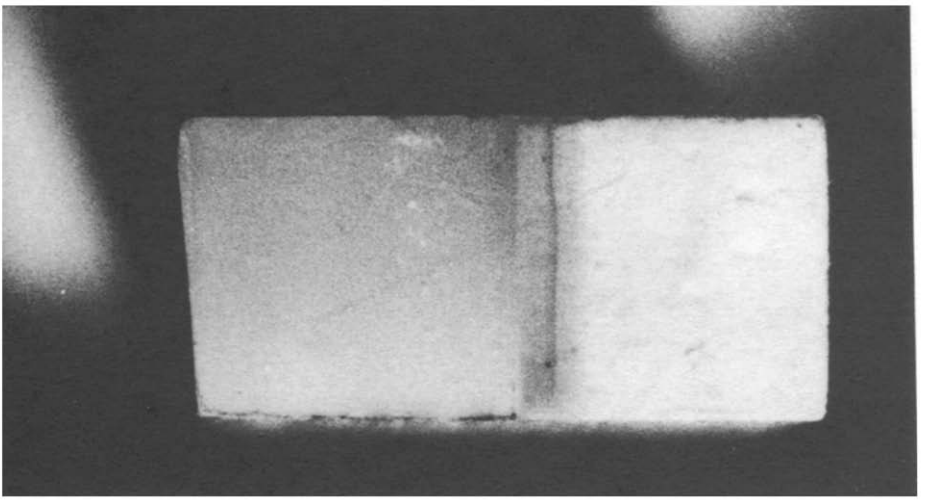

(a)

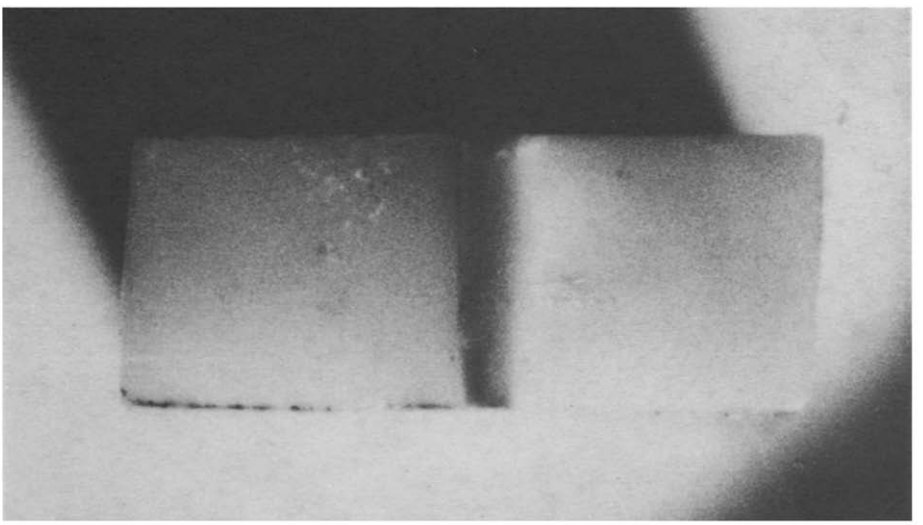

(b)

Fig. 3. Typical fracture surface of ABS specimens: (a) room temperature pendulum-broken samples; (b) liquid air-cooled pendulum-broken samples.

zone is smaller since none or very little whiteness appeared because of the brittle fracture.

Even if the results are superimposed on the same dispersion band, as is shown in Fig. 4, the crack growth was neater for the first procedure. Thus, all subsequent measurements were performed by applying the first procedure.

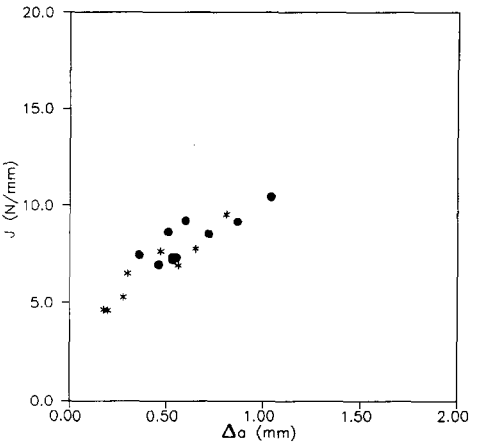

Fig. 4. *J*-values obtained by breaking samples on the pendulum at room temperature (●) or first cooled down in liquid air (*).

4.2 Fitting of *J–R* curves

The problem of approximating the true regression curve from the scatter plot was solved by using the least squares technique.

In the case of ASTM E813–81, data points were directly regressioned to the line:

$$J = a + b\,\Delta a$$

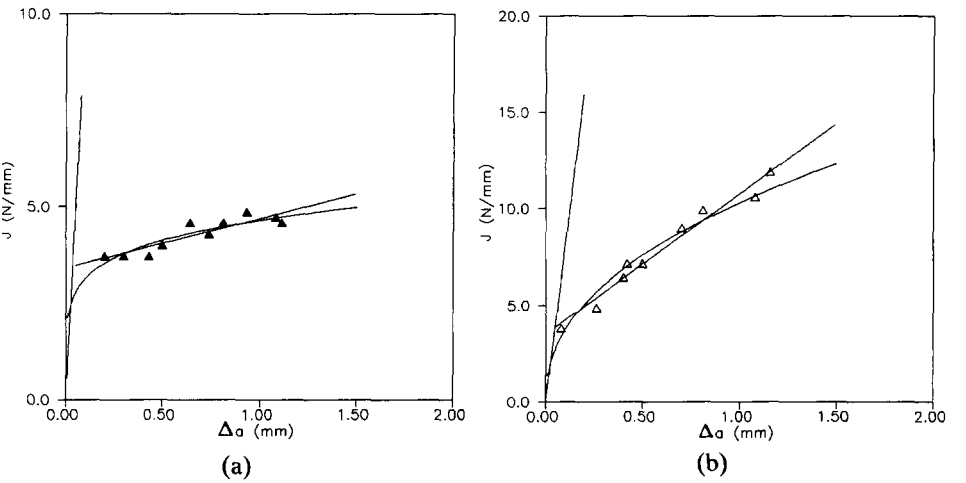

Fig. 5. *J*-values vs. crack growth for data points taken from the literature: (a) Riccò *et al.*[3] (10% RB); (b) Riccò *et al.* (18% RB); (c) Riccò *et al.* (40% RB); (d) Riccò *et al.* (50% RB); (e) Narisawa and Takemori; (f) Zhang *et al.* (ABS I); (g) Zhang *et al.* (ABS II).

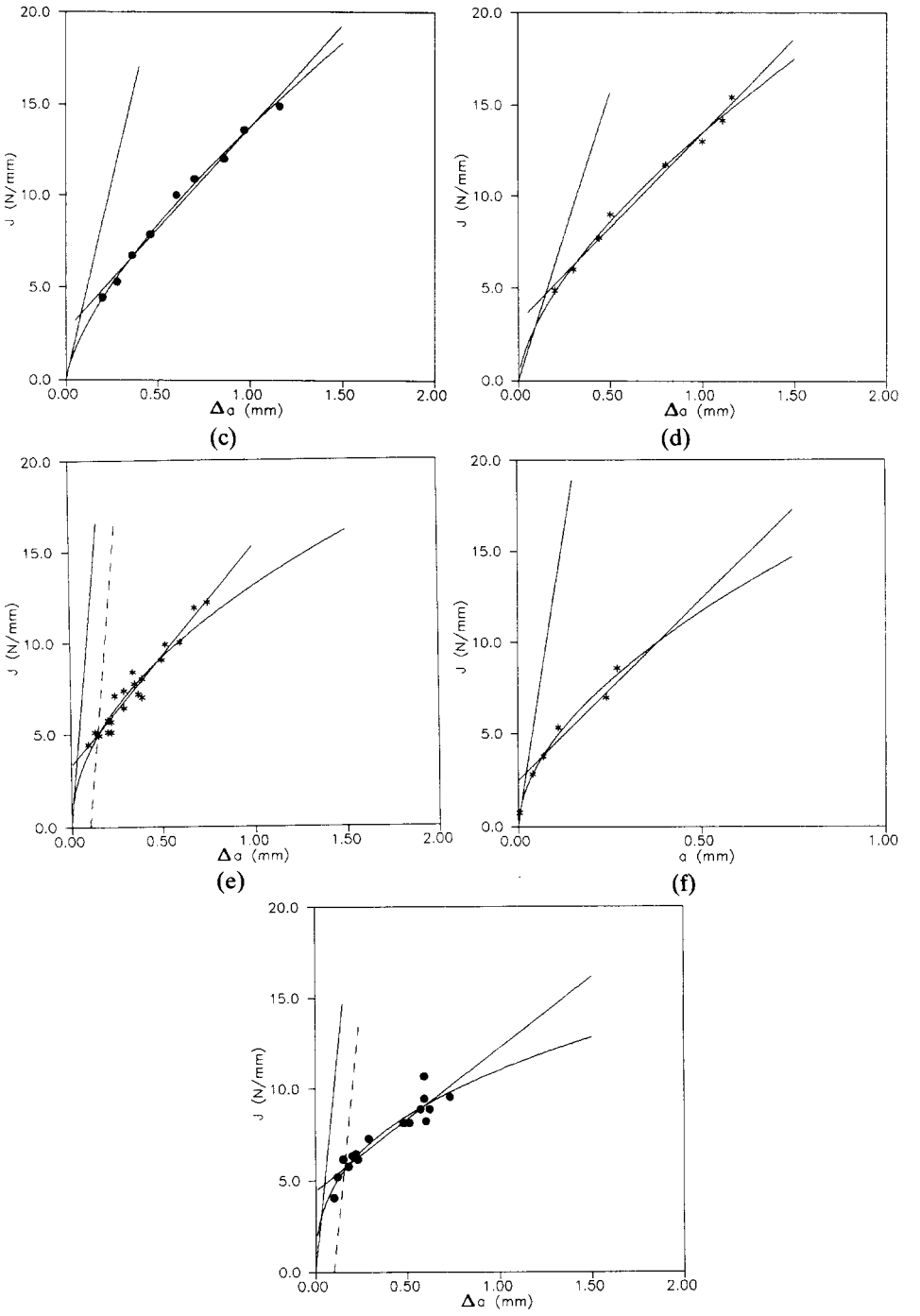

Fig. 5. – *contd.*

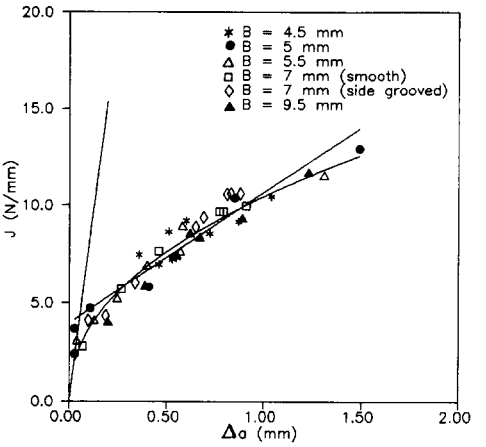

Fig. 6. J-values vs. crack growth for different thickness data points.

In the case of ASTM E813–87, data points were regressioned to the logarithmic transformed exponential expression:

$$\ln J = \ln C_1 + C_2 \ln \Delta a$$

Both forms of data analysis were performed on our data as well as on data reported by other authors for similar resins.[3–5] Figures 5 and 6 show, respectively, the fitting of the experimental values reported in the literature and our data.

4.2.1 *Blunting line*

Some tests were terminated before the onset of the crack advance. The resulting points fell approximately on the theoretical blunting line (Fig. 6):

$$J = 2\sigma_y \, \Delta a$$

It appears to be more or less asymptotic to the exponential J–R fitted curve.

4.3 Model testing

One way of corroborating whether a model is appropriate or not is by residuals examination.[10] Residuals are defined as the n differences:

$$e_i = Y_i - \overline{Y}_i, \qquad i = 1, 2, \ldots, n$$

Y_i (in our investigation J or $\ln J$) is an observation and $\overline{Y}_i$ is the corresponding fitted value obtained by use of the fitted regression

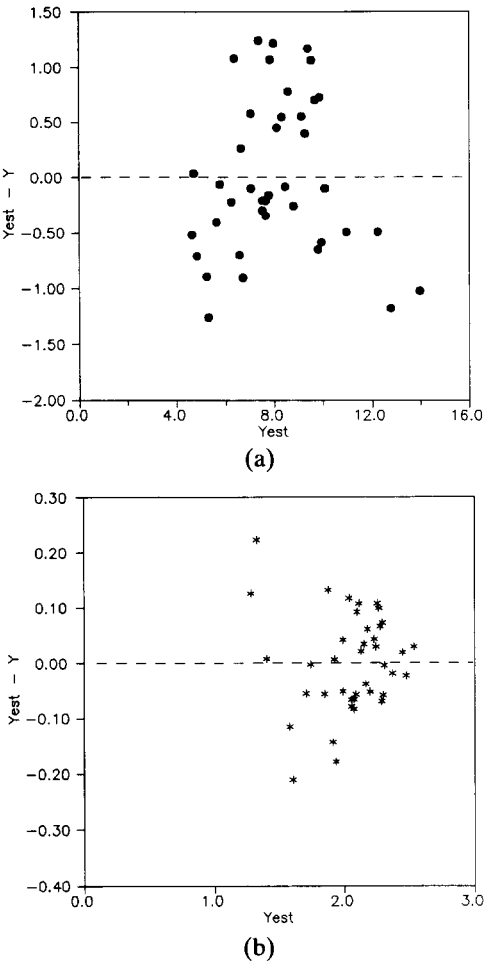

Fig. 7. Residual analysis for different thickness data points: (a) linear fitting; (b) power law fitting.

equation. Linearity is checked by plotting residuals against the predicted Y values.

Although this analysis was made for every case studied, including data from other authors, only one plot is shown as an example in Fig. 7. No systematic pattern was found for any of the fittings. The random scatter about the horizontal line $C = 0$ reflects the linear relationship.

The other statistics analyzed were the coefficient of determination,[11] r^2. It indicates the proportion of variability in Y, explained by the linear relationship, to the independent variable X (in our investigation Δa).

The factor r^2 has the following expression.

$$r^2 = 1 - \frac{E(Y-\bar{Y})^2 - [E(X-\bar{X})(Y-\bar{Y})]^2/E(X-\bar{X})^2}{E(Y-\bar{Y})^2}$$

The coefficient of determination was also calculated for all the data analyzed, including data from other authors, for the two proposed fittings.

Table 1 shows the results. As for every case, r^2 is relatively close to 1, so most of the variability is accounted for by the relationship. Hence, Y is a useful predictor for both cases, leading to a good association between the variables.

This brief statistic analysis shows that there is no reason to reject any one of the fitting procedures, and thus both approaches appear reasonably adequate.

4.4 ASTM E813–81 J_{IC} vs. ASTM E813–87 J_{IC}

Table 1 also shows J_{IC} results calculated by following the two procedures analyzed for both our data and data from the literature.[3–5] The two critical initiation values for the same set, J_{IC} appear substantially different from each other.

J_{IC-87} values are less conservative than J_{IC-81} values, being about 150% larger. Furthermore, Huang[12] had found the same trend in J_{IC-87} and J_{IC-81} values for the case of rubber-toughened polyamides, with greater differences.

TABLE 1
Critical Initiation Factor and Correlation Coefficients

Source	*Material*	J_{IC-81} *(N/mm)*	r^2 *(linear regression)*	J_{IC-87} *(N/mm)*	r^2 *(power law)*
Riccò *et al.*[3]	ABS 10% BR	3·46	0·81	3·64	0·81
	ABS 18% BR	3·85	0·97	5·79	0·95
	ABS 40% BR	3·52	0·98	6·48	0·99
	ABS 50% BR	4·63	0·99	8·05	0·99
Narisawa and Takemori[4]	ABS	3·30	0·94	8·10	0·99
Zhang *et al.*[5]	ABS I	4·80	0·94	7·80	0·91
	ABS II	6·00	0·87	7·70	0·91
In this paper	ABS HR 850	4·31	0·90	5·75	0·91

4.5 Different geometric relationship

4.5.1 *Size requirements*

In some cases, specimens of different thicknesses exhibit different initiation fracture–mechanic parameters. This behavior is the result of a variation in the ratio of plane stress to plane strain constraint at the crack tip.

The use of side-grooves improves plane strain conditions at the crack tip and is generally recommended when results do not fall into plane strain size criterion.

Results regarding thickness variation and side-grooved specimens are shown in Fig. 6. All the data were scattered in the same dispersion band, leading to the same fitted J–R curves within the scanned thickness range, thus confirming a stress state very similar to plane strain condition at the crack tip. Size requirements have been calculated for each of the tests. All the cases, even 4·5 mm thick specimens, met the size conditions, and thus the initiation value J_Q could be taken as the critical plane strain initiation value J_{IC}.

4.5.2 *Initial crack-to-depth ratio*

Results for different initial crack-to-depth ratios are shown in Fig. 8. The fitting was done using exclusively data conforming to the metal ASTM standard E813 recommendations ($0{\cdot}5 < a/W < 0{\cdot}75$) by the exponential approximation.

Nevertheless, data points for a/W equal to 0·4 and 0·8 are superimposed on the same fitted J–R curve. On the other hand, data points for $a/W = 0{\cdot}3$ fall outside the scatter band because this set is not deeply

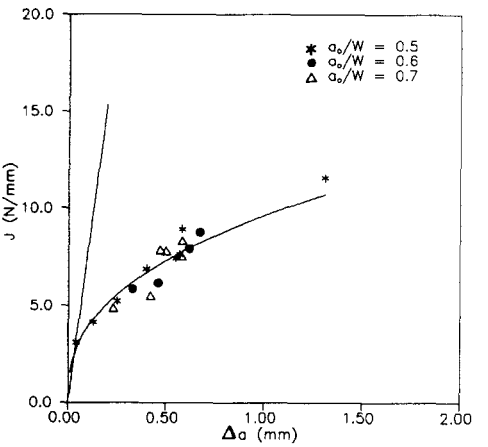

Fig. 8. J-values vs. crack growth for different crack depth-to-width ratio data points.

notched ($a/W > 4$). This condition implies that the plastic calibration factor, η_p, is equal to the elastic calibration factor, η_e, and equal to 2. In this case, η_e is 1·7[13] and this difference leads to the incorrect value calculated with the approximate expression:

$$J = \frac{2U}{B(W-a)}$$

Therefore, in this case the differentiation between elastic and plastic energy should be made.

4.6 Different thickness-to-depth ratios

In addition, the standards suggest that B/W is equal to 0·5, although other relationships are allowed. Results regarding thickness-to-depth ratio variations are shown in Fig. 9. All B/W data seem to fit the same J-R curve.

In every case, size conditions were calculated and found to meet the requirements.

4.7 Exclusion lines

Results regarding the use of different exclusions lines are shown in Fig. 10.

As the problem of applying the exclusion lines criteria was closely related to the thickness of the specimens, data points for every specimen were fitted individually.

It was impossible to apply the criterion to 4·5 and 7 mm thick specimens since an insufficient number of data points fell inside the

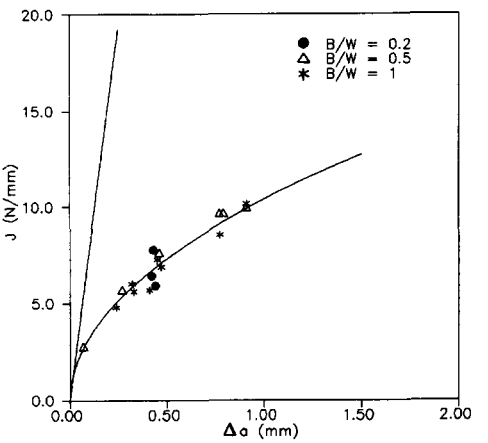

Fig. 9. J-values vs. crack growth for different thickness-to-width ratio data points.

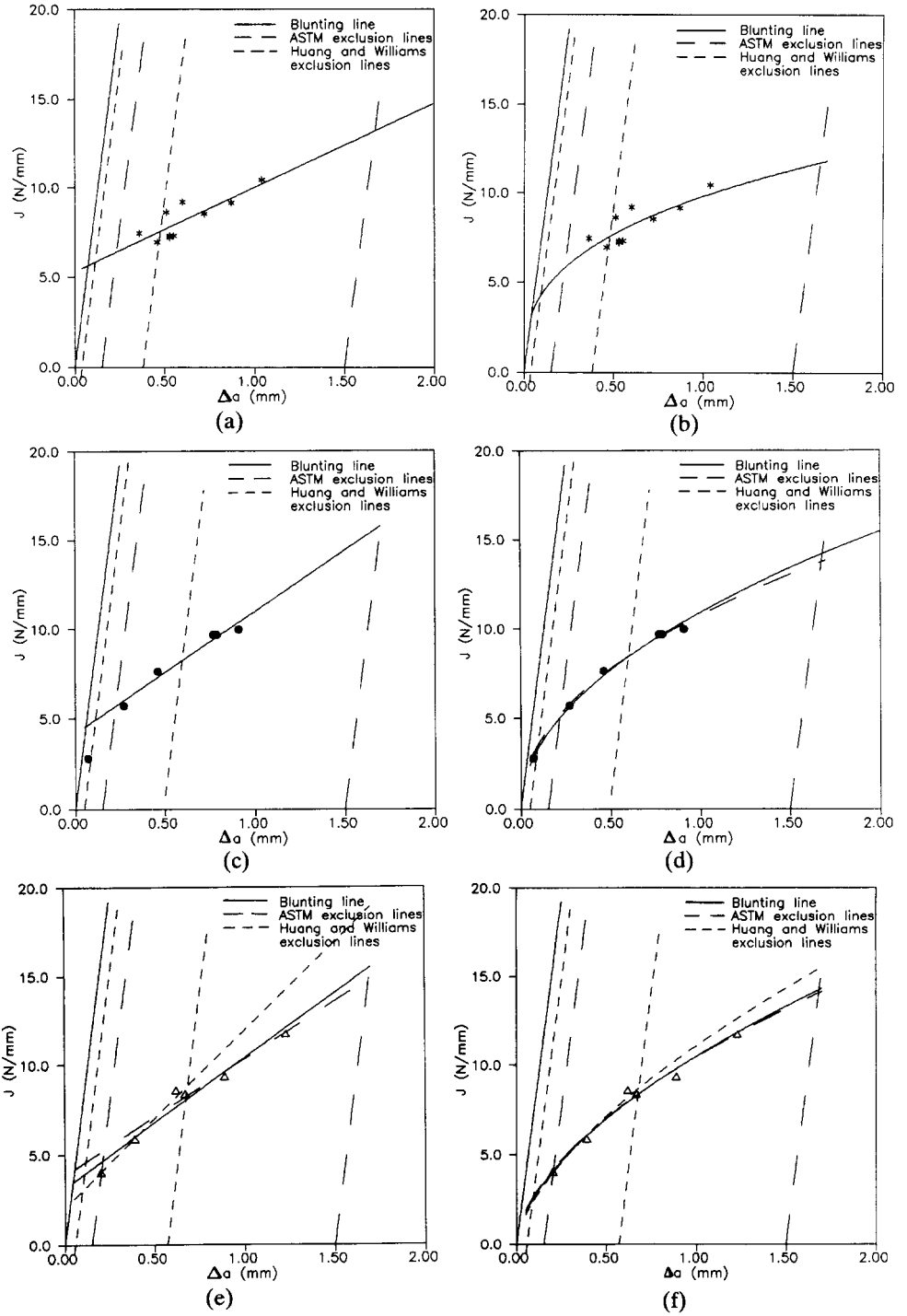

Fig. 10. Data fitted between different 'exclusion lines criteria'. (a) 4·5 mm thick specimens—linear fitting; (b) 4·5 mm thick specimens—power law fitting; (c) 7 mm thick specimens—linear fitting; (d) 7 mm thick specimens—power law fitting; (e) 9·5 mm thick specimens—linear fitting; (f) 9·5 mm thick specimens—power law fitting.

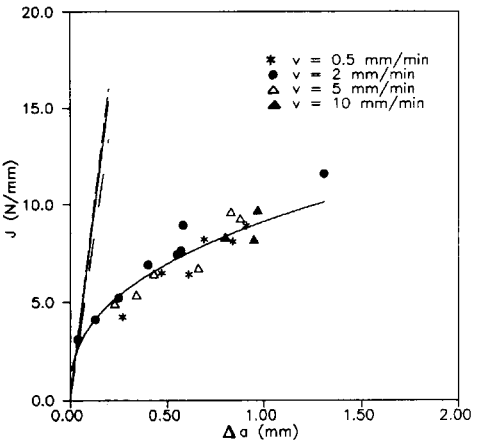

Fig. 11. J-values vs. crack growth for different displacement rate data points.

window limited by the exclusion lines. The other two ways fitting data led to practically the same result.

For 9·5 mm thick specimens the three criteria were applied. The three Power law curves were slightly different, leading to practically the same J_{IC} values. Greater differences were found for linear fitting, leading to different J_{IC} values. The Huang criterion[12] led to the most conservative J_{IC} although it can not be taken as a general result.

4.8 Crosshead displacement rate

Figure 11 shows experimental data for ABS 850, obtained by varying the displacement crosshead rate. Again, data points are scattered within the same dispersion band for the range of displacement rates. Nevertheless, σ_y has a certain dependence upon displacement rate as shown in Table 2. The change in the blunting line slope has a negligible effect on J_{IC} determination, confirming Schapery's[14] assumption (frac-

TABLE 2
Yield Stress as a Function of Crosshead Displacement Rate

σ_y (*MPa*)	*Crosshead speed* (*mm/min*)
33·60	0·5
38·90	2·0
40·13	5·0
40·19	10·0

ture energy is independent of the crack growth rate) within the test rates scanned in this paper. The same result was found by Ricco *et al.*[3]

5 CONCLUSIONS

ABS 850 J-values measured by following the experimental methodology proposed in this paper behaved consistently, leading to R-curves similar to those obtained by other authors on similar resins.[3–5]

Results appear to be independent of geometry and test rate, within the analyzed ranges.

Both ASTM E813–81 and ASTM E813–87 based fittings performed reasonably well on our data and on data from other authors.[3–5]

Exclusion lines recommend by Huang and Williams[8] appear to be too restrictive and practically inapplicable for the case of relatively thin specimens. At the same time, data points within the valid region proposed by ASTM standards gave a reasonable fitting for this type of resin ASTM E813–81 leads to more conservative J_{IC} values. When comparing materials behavior either of the two procedures seems to be adequate.

ASTM E813–81 tries to find a 'true initiation J value,' extrapolating the results at the initiation of crack advance. Yet, from an engineering design point of view we agree with Huang[12] that the ASTM E813–87 standard appears to be the more promising one.

Experience on metals[15] shows that J_{IC} is often a very conservative approach since it makes no use of the reserve in safety due to the rise in crack growth resistance while increasing stable crack extension. Thus, there is a growing trend to design parts allowing for some stable crack extension. This agrees with the ASTM E813–87 standard, which avoids the definition of initiation value by predetermining an arbitrary amount of stable crack growth as an initiation criterion.

Future research should aim to assess the validity of the J_{IC}, determined following different initiation criteria, in predicting the service behavior of plastic structural parts.

ACKNOWLEDGEMENTS

The authors gratefully acknowledge the financial support provided by the Fundación Antorchas and the Third World Academy of Sciences. Also, the authors thank Monsanto Argentina S. A. for supplying materials.

REFERENCES

1. Rice, J. R., A path independent integral and the approximative analysis of strain concentration by notches and cracks. *J. Appl. Mech.*, **35** (1968) 379–86.
2. Chan, M. K. V. & Williams, J. G., J-integral studies of crack initiation of a tough high density polyethylene. *Int. J. Fracture*, **23** (1983) 145–9.
3. Riccò, T., Rink, M. Caporusso, S. & Pavan, A., An analysis of fracture initiation and crack growth in ABS resins. In *Proceedings of the International Conference on 'Toughening of Plastics II'* London, 2–4 July 1985, The Plastic's & Rubber Institute, 27/1–27/9.
4. Narisawa, I. & Takemori, M. T., Fracture Toughness of Impact-Modified Polymers Based on the *J*-integral. *Polym. Eng. Sci.*, **29** (1989) 671–8.
5. Zhang, M. J., Zhi, F. X. & Su, X. R., Fracture Toughness and Crack Growth Mechanism for Multiphase Polymers. *Polym. Eng. Sci.*, **29** (1989) 1142–6.
6. Landes, J. D. & Begley, J. A., Test results from *J*-integral studies: An attempt to establish a J_{IC} testing procedure. ASTM STP 560, American Society for Testing and Materials, Philadelphia, (1974) 170–86.
7. Rice, J. R., Paris, P. C. & Merkle, J. G., Some further results on *J* integral analysis and estimates. ASTM STP 536, American Society for Testing and Materials, Philadelphia, 1973, 231–45.
8. Huang, D. D. & Williams, J. G., *J* testing of toughened nylons. *J. Mater. Sci.*, **22** (1987) 2503–8.
9. Ward, J. M., Review: The yield behaviour of polymers. *J. Mater. Sci.*, **6** (1971) 1397–417.
10. Dowdy, S. & Wearden, S., *Statistics for Research*, John Wiley, New York, 1983, chp. 9, p. 215.
11. Dowdy, S. & Wearden, S., *Statistics for Research*, John Wiley, New York, 1983, chp. 9, p. 230.
12. Huang, D. D., In situ crack growth studies of toughened polymers. *Proc. ACS Div. Polym. Mater. Sci. Eng.*, **63** (1990) 578–82.
13. Vedia, L. A. de, *Mecánica de Fracturas*, Proyecto Multinacional de Investigación y Desarrollo en Materiales OEA–CNEA, Buenos Aires, 1986, p. 116.
14. Shapery, R. A., A theory of crack initiation and growth in viscoelastic media. II Approximate methods of analysis. *Int. J. Fracture*, **11** (1975) 369–88.
15. Cayard, M. S. & Bradley W. L., A comparison of several analytical techniques for calculating *J–R* curves from load displacement data and their relation specimen geometry. *Eng. Fracture Mech.*, **33** (1989) 121–32.